Received: 26 May 2022 | Revised: 26 October 2022 | Accepted: 28 November 2022

DOI: 10.1002/ecy.3967

ARTICLE

ECOLOGY
ECOLOGICAL SOCIETY OF AMERICA

Optimal energy allocation trade-off driven by size-dependent physiological and demographic responses to warming

Viktor Thunell[1] | **Anna Gårdmark**[1] | **Magnus Huss**[1] | **Yngvild Vindenes**[2]

[1]Department of Aquatic Resources, Swedish University of Agricultural Sciences, Uppsala, Sweden

[2]Centre for Ecological and Evolutionary Synthesis (CEES), Department of Biosciences, University of Oslo, Oslo, Norway

Correspondence
Viktor Thunell
Email: viktor.thunell@slu.se

Funding information
Research Council of Norway, Grant/Award Number: 244404; Swedish Research Council, Grant/Award Number: 2015-03752

Handling Editor: Lorenzo Ciannelli

Abstract

Body size–dependent physiological effects of temperature influence individual growth, reproduction, and survival, which govern animal population responses to global warming. Considerable knowledge has been established on how such effects can affect population growth and size structure, but less is known of their potential role in temperature-driven adaptation in life-history traits. In this study, we ask how warming affects the optimal allocation of energy between growth and reproduction and disentangle the underlying fitness trade-offs. To this end, we develop a novel dynamic energy budget integral projection model (DEB–IPM), linking individuals' size- and temperature-dependent consumption and maintenance via somatic growth, reproduction, and size-dependent energy allocation to emergent population responses. At the population level, we calculate the long-term population growth rate (fitness) and stable size structure emerging from demographic processes. Applying the model to an example of pike (*Esox lucius*), we find that optimal energy allocation to growth decreases with warming. Furthermore, we demonstrate how growth, fecundity, and survival contribute to this change in optimal allocation. Higher energy allocation to somatic growth at low temperatures increases fitness through survival of small individuals and through the reproduction of larger individuals. In contrast, at high temperatures, increased allocation to reproduction is favored because warming induces faster somatic growth of small individuals and increased fecundity but reduced growth and higher mortality of larger individuals. Reduced optimum allocation to growth leads to further reductions in body size and an increasingly truncated population size structure with warming. Our study demonstrates how, by incorporating general physiological mechanisms driving the temperature dependence of life-history traits, the DEB–IPM framework is useful for investigating the adaptation of size-structured organisms to warming.

Ecology. 2023;104:e3967.
https://doi.org/10.1002/ecy.3967

KEYWORDS
adaptation, body growth, climate change, DEB–IPM, fish, reproductive investment, size structure, temperature-size rule, trade-off

INTRODUCTION

Predicting how animal populations will respond to climate warming requires knowledge of how environmental temperature drives not only physiological and ecological responses but also adaptation. This includes consideration of how temperature affects fitness, via growth, reproduction, and survival of individuals, depending on life-history trade-offs (Ahti et al., 2020; Fryxell et al., 2020; Kozlowski et al., 2004; Stearns, 1992). Because reproductive output and survival are commonly linked to body size, the trade-off in energy allocation between somatic growth and reproduction is particularly relevant for adaptation under climate change (Barneche et al., 2018; Post & Parkinson, 2001; Ward et al., 2017).

Changes in somatic growth rate and body size with warming may reflect both the direct effects of environmental temperature on growth and adaptive responses to changing selection pressures through other parts of the life cycle, correlated with growth (Audzijonyte et al., 2018; Daufresne et al., 2009; Fryxell et al., 2020; Loisel et al., 2019). In ectotherms, warming often causes faster growth and development early in life but reduced adult or maximum body sizes, truncating the population size distribution and decreasing the average body size (Atkinson, 1994; Baudron et al., 2014; Forster & Hirst, 2012; Huss et al., 2019). The temperature dependence of metabolic processes couples such effects to net available energy its body size dependence size dependence (Huey & Kingsolver, 2019; Ohlberger et al., 2011). Importantly, metabolic maintenance costs increase with temperature and, in particular for larger individuals, decrease growth rates at higher temperatures (Christensen et al., 2020; Lindmark et al., 2022). However, given sufficient food availability, warming can increase growth rates of smaller individuals due to size- and temperature-dependent effects on consumption. Such size-dependent physiological effects of temperature affect the size structure, dynamics, and life history of animal populations (Huss et al., 2019; Ikpewe et al., 2020; van der Sleen et al., 2022; Wang et al., 2020). Implicit in these findings is that temperature affects the size dependence of allocable energy, so that different allocation strategies may be favored by natural selection depending on temperature (Kozlowski et al., 2004). Accordingly, experimental evidence shows that distinguishing between these selective effects of temperature on somatic growth and reproduction can help predict how warming will affect evolutionary trade-offs in energy allocation (Fryxell et al., 2020; Loisel et al., 2019; Ward et al., 2017; Wootton et al., 2022). However, current predictions lack the explicit links between body size–dependent effects of temperature on net energy gain, subsequent demographic processes (e.g., survival and reproduction), and evolutionary responses to changing selection on these processes (Koenigstein et al., 2016).

Since survival and reproduction are often size dependent, changing the energy allocation between growth and reproduction also changes age-specific survival, influencing fitness and lifetime reproductive success (Gunderson, 1997; Law, 1979; Roff et al., 2006). When mortality decreases with size, for instance due to reduced predation risk, a high somatic growth rate can increase survival early in life (Pepin, 1991; Werner & Gilliam, 1984) and favor future reproductive success (Perrin & Sibly, 1993). Consequently, energy allocation to reproduction increases strongly with body size in many species with indeterminate growth (Arendt, 2015; Barneche et al., 2018; Marshall & White, 2019), reflecting such an adaptive strategy (Audzijonyte & Richards, 2018; Heino & Kaitala, 2001; Kozlowski, 1997). As warming can alter the conditions for such trade-offs via size-dependent effects on growth rates, fecundity, and survival, the optimal strategy of energy allocation to somatic growth versus reproduction will also shift. For example, if the effects of warming on growth and survival are positive for small individuals but negative for large individuals (Baudron et al., 2014; Ikpewe et al., 2020; Lindmark et al., 2022; Pepin, 1991; Thorson et al., 2017), this would decrease the fitness cost of energy allocation to reproduction early in life and increase the fitness cost of growing large. We currently lack knowledge of how size and temperature interact to determine the costs and benefits of energy allocation via demographic processes.

Here we ask how mean temperature affects the optimal strategy for the allocation of energy to somatic growth contra reproduction and how the selection pressure on the optimal allocation via different demographic processes changes with size. To this end, we construct a dynamic energy budget integral projection model (DEB–IPM) (Easterling et al., 2000; Kooijman, 1993). This model links size- and temperature-dependent individual consumption and maintenance rates via energy allocation, annual somatic growth, and reproduction to population growth rate (mean fitness) and size structure. Model structure and parameterization are based on a population of northern pike (*Esox lucius*), an opportunistic freshwater predator (Le Cren, 2001).

We identify the energy allocation strategy that maximizes mean fitness (long-term population growth rate, λ) for a given temperature and study this over a range of temperatures. Furthermore, we assess the respective contributions of growth, fecundity, and survival at different sizes to the selection pressure on optimal allocation at different temperatures. These analyses identify how selection pressure with respect to energy allocation may shift with temperature throughout the life cycle.

METHODS

We model the physiological effects of warming on optimal energy allocation to somatic growth contra reproduction using a combination of dynamic energy budget (DEB) theory (Kooijman, 1993) and the integral projection model framework (IPM) (Easterling et al., 2000; Ellner et al., 2016). DEB theory enables a straightforward model of growth rates of soma and reproductive reserves, dependent on energy allocation and on individual consumption and maintenance rates varying with body size and temperature. The IPM framework, on the other hand, uses size-dependent demographic functions (growth, fecundity, survival, and offspring size) to project changes in the population size distribution in discrete time. For a density-independent IPM we can calculate the asymptotic properties of the long-term population growth rate (mean fitness) and stable size distribution. In our DEB–IPM, we use general mass- and temperature-dependent functions of physiological rates to inform the DEB model, in which daily rates integrated over a growing season define the annual demographic functions in the IPM. We use data from northern pike (*E. lucius*) in the UK's lake Windermere (Le Cren, 2001; Winfield et al., 2013a, 2013b; Winfield & Fletcher, 2013) and experimental data on temperature effects on fish metabolism and consumption rates to parameterize the model (Table 1). Using this temperature-dependent DEB–IPM, we assess how temperature affects optimal energy allocation (via the allocation parameter κ_0). In what follows, we will describe the model functions, from the DEB model (Equations 1–7c) to demographic functions (Equations 9, 10, and 12–15) to the projection function of the IPM (Equations 8a and 8b), and our analyses of the resulting DEB–IPM.

Individual level: Mass- and temperature-dependent consumption and maintenance rates

We model the temperature (T) and body size (mass, m) dependencies of the energy budget of individuals using allometric functions of maintenance (M) and consumption (C) rate (in grams per day, [$\mathrm{g\,day^{-1}}$]), combined with functions that model temperature effects $r_{C,M}(T)$:

$$M(m, T) = \rho_1 m^{\rho_2} r_M(T), \tag{1}$$

$$C(m, T) = \varepsilon_1 m^{\varepsilon_2} r_C(T), \tag{2}$$

where $\rho_{1,2}$ and $\varepsilon_{1,2}$ are the allometric scalars and exponents for maintenance and consumption, respectively (Appendix S1: Figure S1a). By measuring consumed energy and metabolism in $\mathrm{g\,day^{-1}}$ and somatic growth and reproductive output in grams (see following discussion), we assume that the different body tissues and all consumed food contain the same amount of energy per gram.

We use the Boltzmann–Arrhenius equation (Equation 3) to model the activation (increase) in maintenance rate with temperature (Appendix S1: Figures S1.1b and S1.2, Clarke & Fraser, 2004; Gillooly et al., 2001). Consumption rate (Equation 4) is considered unimodal over temperature (Englund et al., 2011) and is therefore modeled using the Sharpe–Schoolfield equation (Schoolfield et al., 1981), expressed as a rearranged version of that by Padfield et al. (2020) (Appendix S1: Figure S1.1b):

$$r_M(T) = e^{E_{AM}(T - T_0)/(kTT_0)}, \tag{3}$$

$$r_C(T) = C_{T_0} e^{E_{AC}(T - T_0)/(kTT_0)} \times \left(1 + e^{\frac{E_{DC}(T - T_D)}{kTT_D}}\right)^{-1}, \tag{4}$$

where $E_{AC,M}$ and E_{DC} are the activation and deactivation energies, respectively, determining temperature sensitivity, and k is the Boltzmann constant ($8.617 \times 10^{-5}\,\mathrm{eV\,K^{-1}}$). The difference between the current (T, in Kelvin) and reference temperature (T_0) sets the exponent or size of the temperature effect for activation. The analogous effect for deactivation is the difference between the current temperature (T) and temperature at which half the rate is reduced due to high temperatures (T_D). The biological interpretation of T_D relates biological processes to enzymatic activity and is the temperature where enzymes are half active and half inactive due to high temperatures (Hultin, 1955; Schoolfield et al., 1981). C_{T_0} scales the temperature effect on the consumption rate at the reference temperature (Lindmark et al., 2022; Padfield et al., 2020).

Individual level: DEB model

The DEB describes the daily rates of energy uptake and use for individual somatic growth, maintenance costs

TABLE 1 Parameter values for mass and temperature dependence of consumption and maintenance rate and for functions used in dynamic energy budget integral projection model (DEB–IPM).

Parameter	Value	Unit	Description	Reference
Mass- and temperature-dependent consumption and maintenance				
ε_1	0.94	$g^{1-\varepsilon_2}\ day^{-1}$	Allometric constant of consumption rate	Free parameter
ε_2	0.47	…	Allometric exponent of consumption rate	Free parameter
ρ_1	0.02	$g^{1-\rho_2}\ day^{-1}$	Allometric constant of maintenance rate	Armstrong et al. (1992), Lindmark et al. (2019)
ρ_2	0.76	…	Allometric exponent of maintenance rate	Armstrong et al. (1992), Lindmark et al. (2019)
T_0	292	K	Reference temperature for maintenance and consumption rate	Lindmark et al. (2019)
T_D	292.75	K	Temperature at which half the rate is reduced due to temperature	Lindmark et al. (2022)
E_{AI}	0.73	eV	Activation energy consumption	Lindmark et al. (2022)
E_{dI}	1.89	eV	Deactivation energy consumption	Lindmark et al. (2022)
E_{AM}	0.62	eV	Activation energy maintenance	Lindmark et al. (2022)
C_{T_0}	1.83	$g\ day^{-1}$	Consumption rate at T_0	Lindmark et al. (2022)
k	8.61733×10^{-5}	$eV\ K^{-1}$	Boltzmann constant	
DEB				
κ_0	0.89 and varied	…	Allocation for mass = 0/Intercept—Energy allocation	Free parameter
κ_m	2.82	…	Rate constant/Slope—Energy allocation	Free parameter
α	0.4	…	Assimilation efficiency	Diana (1983), Wieser and Medgyesy (1991)
s_l	183	days	Growing season length	April to September
m_{mat}	417	g	Maturation size	Calculated from maturation length in Vindenes et al. (2014)
IPM				
e_m	0.00351	g	Egg mass	Winfield et al. (2013a)
o_{surv}	1.9×10^{-4}	…	Survival constant for egg to age 1	Kipling and Frost (1970), Vindenes et al. (2014)
$\sigma_o{}^2$	48.1256	…	Standard deviation age 1 size	Winfield et al. (2013b)
	1000	…	Matrix mesh size	
τ_g	300	…	Factor, growth standard deviation function	Free parameter
ν_g	−0.0001	…	Exponent, growth standard deviation function	Free parameter
a_1	66.96397	…	Parameters for size- and temperature-dependent survival	Vindenes et al. (2014)
a_2	0.2904			
a_3	15.75566			
a_4	0.1707			
a_5	0.0448			
a_6	0.1931			

and reproductive reserve (Equations 6a–6c and 7a–7c, Appendix S1: Section S1 for graphic description). The consumption function $C(m, T)$ and assimilation efficiency α determine energy uptake, and the maintenance function $M(m, T)$ determines the energetic costs of metabolism (assuming that maintenance cost equals standard metabolic rate). The standard DEB model (Kooijman, 1993) also contains a feeding level (Y). We scale consumption using an allometric scalar (ε_1), making Y redundant, so we exclude it from our model. In the standard DEB model, the parameter κ (taking values from 0 to 1) determines the relative allocation of energy to maintenance and somatic growth versus reproduction. Here, we instead use a normalized exponential mass-dependent function to model a decreasing allocation of energy to growth with increasing size:

$$\kappa(m) = \kappa_0 e^{-m/(\kappa_m \times 20{,}000)}, \tag{5}$$

where κ_0 is the energy proportion allocated to growth and maintenance for an individual with zero mass (or intercept), κ_m is the rate constant (or slope, Appendix S1: Figure S1.1c), and 20,000 is the maximum of the size interval in the IPM (see *Analyses*). As maintenance costs increase with size, growth declines and the standard κ--dependent DEB model predicts that energy allocated to reproductive reserves, which is a function of (a sublinear) consumption rate (Appendix S1: Figure S1.1a), will decrease exponentially with size. This, however, does not fit observations in many ectotherm animal populations, and especially not for fish where reproductive energy investment increases strongly with size, making reproduction increasingly prioritized over growth (Barneche et al., 2018; Honěk, 1993; Marshall & White, 2019). This implies a linear or supralinear (hyperallometric) scaling of energy allocation to reproduction, as described by Equation (5) (note that reproductive hyperallometry may not necessarily originate from the allocation strategy but can have physiological or ecological origin, e.g., Potter and Felmy [2022] and Sadoul et al. [2020]). This makes our DEB flexible and more applicable to fish populations. We show the effects of mass-independent, as opposed to mass-dependent, energy allocation to reproductive reserves on growth and fecundity in Appendix S1: Section S3. Furthermore, we assume that juveniles use the "reproductive" energy for development or storage, whereas mature individuals allocate it to reproduction (Kooijman, 1993), meaning that allocation to reproduction from the energy budget $(1-\kappa(m))$ holds throughout ontogeny.

Maintenance costs and consumption gains determine the conditions for somatic growth (Equations 6a–6c) and reproduction (Equations 7a–7c), depending on size and temperature. When maintenance costs are lower than $\kappa(m)$-scaled assimilated energy (Equations 6a and 7a), the difference between this $\kappa(m)$-scaled assimilated energy and maintenance determines individual change in somatic body mass, whereas allocation to reproduction is the assimilated energy scaled by $1-\kappa(m)$. Energy is channeled from the reproductive reserve to cover maintenance when the maintenance costs exceed the $\kappa(m)$-scaled assimilated energy (Equations 6b and 7b, Corriero et al., 2021; Smallegange et al., 2017). Consequently, the κ-rule makes reproduction equally prioritized to growth and maintenance when energetic conditions are favorable, but reproduction is prioritized over growth when they are not. When maintenance costs are larger than assimilated energy, starvation (shrinking in mass) occurs (Equations 6c and 7c; in our analysis, however, growth will cease before starvation conditions emerge). Accordingly, the somatic growth rate is

$$\frac{dm}{dt} = \kappa(m)\alpha C(m,T) - M(m,T) \text{ if } M(m,T) \le \kappa(m)\alpha C(m,T) \text{ and } m > 1, \tag{6a}$$

$$\frac{dm}{dt} = 0 \text{ if } \kappa(m)\alpha C(m,T) < M(m,T) \le \alpha C(m,T), \tag{6b}$$

$$\frac{dm}{dt} = \alpha C(m,T) - M(m,T) \text{ if } \alpha C(m,T) < M(m,T). \tag{6c}$$

The rate of energy allocation to reproduction is given by

$$\frac{dR}{dt} = (1-\kappa(m))\alpha C(m,T) \text{ if } M(m,T) \le \kappa(m)\alpha C(m,T), \tag{7a}$$

$$\frac{dR}{dt} = \alpha C(m,T) - M(m,T) \text{ if } \kappa(m)\alpha C(m,T) < M(m,T) \le \alpha C(m,T), \tag{7b}$$

$$\frac{dR}{dt} = 0 \text{ if } \kappa(m)\alpha C(m,T) < M(m,T). \tag{7c}$$

The rate functions for growth (Equations 6a–6c) and reproduction (Equations 7a–7c) provided by the DEB describe daily somatic growth and increase in reproductive reserve, respectively, and temperature-dependent size at age 1 year. We approximate these quantities numerically with time integrations of the DEB (using the function ode() at the default settings [Soetaert et al., 2010] in R version 4.0.3 [R Core Team, 2020]). Note that this approach differs from the DEB–IPM proposed by Smallegange et al. (2017), in which the integration of the differential equation for the growth rate is solved analytically to estimate von Bertalanffy growth equation parameters, whereas growth herein varies with size- and temperature-dependent net energy gain and allocation (see *Discussion*).

Population level: Study system

We aim to build a general framework to analyze temperature effects on allocation strategies in ectotherms but acknowledge that parameters, and therefore allocation strategies, vary within and among species. We therefore showcase the DEB–IPM and analysis for the Windermere pike (Le Cren, 2001). Previous studies assessed several aspects of the individual- and population-level temperature dependence of Windermere pike using female length-based IPMs built from statistical models of demographic functions (Vindenes et al., 2014, 2016). Our weight-based DEB–IPM takes a more mechanistic approach by letting the underlying DEB models define the demographic functions describing growth, reproduction, and survival between years. Model parameters (Table 1) are determined from empirical estimates of class-, species-, or population-specific parameters when appropriate and from estimating the allometric functions in the DEB model to fit the observed growth and fecundity of Windermere pike (see Appendix S1: Section S2). The DEB–IPM thus enables a physiological foundation to study the effects of temperature on long-term fitness and its sensitivity to main parameters.

Northern pike is a spring-spawning capital breeder that breeds annually in Windermere (Frost & Kipling, 1967). During the main growing season (April–September), the female pike allocates energy to somatic growth and to reproductive energy reserves that it uses for building up ovaries, mainly in the autumn months (Frost & Kipling, 1967). Most female pike in Windermere reach maturity in spring at age two, and body size is a main predictor of maturity and fecundity (Frost & Kipling, 1967).

Population level: IPM

Our IPM (Figure 1) has two discrete life-history stages: (1) eggs and (2) individuals of age 1 and older, where the latter stage is structured according to the continuous state variable body size (mass, denoted m_s in time s and m_{s+1} in time $s+1$). Each transition between discrete time points ($s \rightarrow s+1$) represents a growing season, from one spring to the next. Population growth depends on four demographic functions, where the first three are constructed from the DEB: next year's size distribution of age 1 individuals $o(m_{s+1};T)$, next year's size distribution of all other individuals $g(m_{s+1};m_s,T)$, next year's fecundity $f(m_s,T)$, and annual survival probability $a(m_s,T)$. Population-level responses to temperature thus emerge from individual demographic processes. Our IPM is density independent and uses a postreproductive census (Rees et al., 2014) at the start of the growing season (right after spawning). The population distribution (eggs plus the number of individuals at different sizes) at time $s+1$ is a function of the distribution at time s:

$$n_0(s+1) = \int_0^{\infty} a(m_s,T) f(m_s,T) n_\Omega(m_s,s) dm_s, \tag{8a}$$

$$n_\Omega(m_{s+1},s+1) = o(m_{s+1};T) n_0(s) o_{\text{surv}} + \int_0^{\infty} a(m_s,T) g(m_{s+1};m_s,T) n_\Omega(m_s,s) dm_s\,. \tag{8b}$$

Equation (8a) describes next year's $(s+1)$ egg production, which is determined by the integral of the fecundity $f(m_s,T)$ of surviving ($a(m_s,T)$, functions described in what follows) and reproducing individuals from this year (s). Next year's population size distribution of individuals of age 1 and older (Equation 8b) consists of individuals resulting from eggs laid in this year $(n_0(s))$ that grow and survive the first year $(o(m_{s+1};T)o_{\text{surv}})$ and individuals of size m_s that survive from this year and grow to a new size $m_{s+1}(a(m_s,T)g(m_{s+1};m_s,T))$, integrated over all sizes m_s.

The distribution of body size in the following year, $g(m_{s+1},m_s,T)$, is assumed to be lognormal and describes the distribution of possible sizes y that an individual of current size m_s can grow to next year (approximates the normal distribution for higher values of m). This function uses the output from numerical integrations of Equation (5) of the DEB growth model to estimate the mean of size m_{s+1} (μ_g) for a given temperature T:

$$\mu_g(m_s,T) = \int_0^{s_l} \frac{dm}{dt} dt, \tag{9}$$

where s_l is the length of the growing season in days. We assume an exponentially decreasing function for the standard deviation of size σ_g as a function of μ_g in the lognormal probability density function where the factor (τ_g) and exponent (ν_g) are free parameters (see Appendix S1: Section S2 for comparison with data):

$$\sigma_g(\mu_g) = \tau_g e^{\nu_g \mu_g}. \tag{10}$$

Yearly survival probability $a(m_s,T)$ is a mass-dependent version of the length- and temperature-dependent logit survival model estimated by Vindenes et al. (2014) for

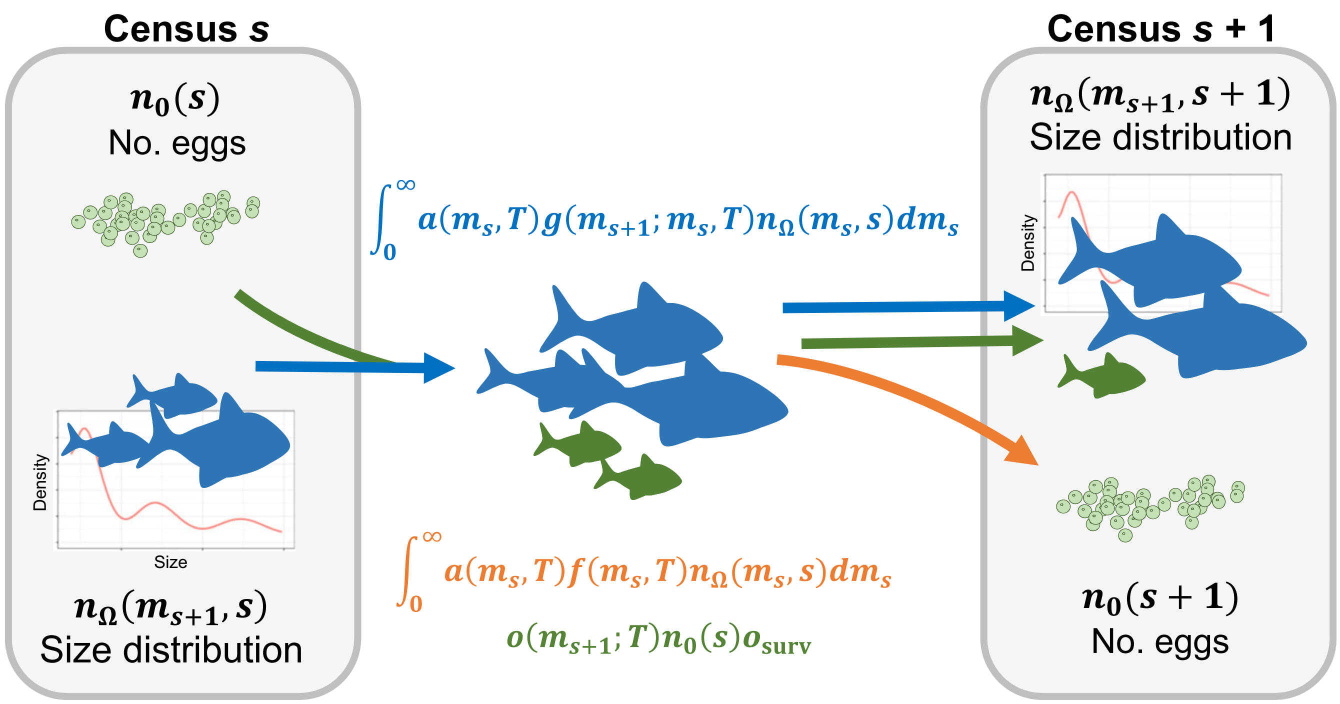

FIGURE 1 Demographic processes in the temperature-dependent dynamic energy budget integral projection model (DEB–IPM) fitted to Windermere pike. The IPM calculates annual changes in the population (consisting of the number of eggs n_0 and the size distribution n_Ω) between census s and $s+1$ depending on the growth and survival of individuals from eggs to age 1 (green) and from age 1 to older fish (blue) and on reproduction from mature fish (orange). In turn, the demographic function distributions of size at age 1 $o(m_{s+1}, T)$, distribution of older individuals (somatic growth) $g(m_{s+1}, m_s, T)$, and fecundity $f(m_s, T)$ are derived from the size- and temperature-dependent DEB, and survival probabilities $a(m_s,T)$ and o_{surv} are based on estimates from Windermere pike.

Windermere pike. We calculated length from weight using our estimated relationship from Windermere pike data as follows (Winfield et al., 2013b):

$$l=\left(\frac{w}{e^{-6.49286}}\right)^{(1/3.4434)} \tag{11}$$

The survival model predicts yearly survival probability between spring and autumn and assumes that winter survival is 1. Size-dependent annual survival probability increases from a small size from $0 < m < \sim 1000$ g and reaches an asymptote of $0.68\,\text{year}^{-1}$ at $T = 287$ K, $m > \sim 1000$ g as follows:

$$a(m_s, T) = \left(1+\exp\left(a_1 - {m_s}^{a_2}\left(a_3 - a_4 {m_s}^{a_2}\right) + T\left(a_5 {m_s}^{a_2} - a_6\right)\right)\right)^{-1},$$

$$m_s < \arg\max_{m_s} a(m_s, T), \tag{12}$$

$$a(m_s, T) = \max_{m_s} a(m_s, T),\ m_s \geq \arg\max_{m_s} a(m_s, T). \tag{13}$$

The fecundity function describes the production of eggs, dependent on energy allocated to reproductive reserve, by females surviving to reproduce and is estimated using numerical time integration of Equations (6a)–(6c) in the DEB. With an even sex distribution, only half of the produced eggs contribute to population growth in our female-based model. We describe the number of eggs produced in spring in $s+1$ (fecundity) per surviving female as

$$f(m_s, T) = 0.5 \times \int_0^{s_l} \frac{dR}{dt} dt \times \frac{1}{e_m}, \tag{14}$$

where dR/dt is the temperature-dependent amount of energy allocated to reproduction (Equations 7a–7c), and e_m is the egg mass.

We also use the DEB model to calculate the mean size at age 1, $\mu_o(e_m, T)$ (first year growth), as a function of temperature and egg mass. In this integral, defining growth from egg to age 1, we reduced the length of the growing season (s_l) to half that of individuals older than 1, thereby also accounting for time of development in efficiently feeding individuals:

$$\mu_o(e_m, T) = \int_0^{s_l/2} \frac{dm}{dt} dt. \tag{15}$$

We estimate the variance of size at age 1 (σ_o^2) using data on back-calculated age and length (converted to weight using the inverse of Equation 11) from opercular bones from Windermere pike (Winfield et al., 2013b). The age 1 size distribution is assumed to follow a lognormal density distribution. The parameter o_{surv} (in Equation 8b) describes the survival of an egg to age 1 and is assumed to be independent of temperature, with the value based on previous estimates in Windermere (Frost & Kipling, 1967; Vindenes et al., 2014). This reflects a deliberate choice to focus our study on how growth, fecundity, and survival emerging from temperature- and mass-dependent growth trajectories (yielded by the DEB model) govern individual energy allocation and population growth and size distribution. We thus disregard the fact that temperature can affect, for example, egg survival (Swift, 1965; Vindenes et al., 2016) and winter mortality (Byström et al., 2006) with effects on population structure and growth (Byström et al., 1998; Vindenes et al., 2014).

Parameterization

We parameterized the DEB–IPM using existing observational data of the Windermere pike and on laboratory experiments on pike or other fish (Table 1). We based the size dependence of maintenance rate on metabolic rate experiments on pike (Armstrong et al., 1992; recalculated by Lindmark et al. [2019]). We are, however, not aware of any data on size scaling of consumption rates for pike. As consumption rates are naturally highly variable, so we instead considered the consumption rate size scaling parameters in the DEB (ε_1 and ε_2) as free and matched modeled growth trajectories and size-dependent fecundity with those in the Windermere pike population (sensu Essington et al., 2001). To this end, we also used the parameters in the allocation function $\kappa(m)$ (κ_0 and κ_m) to replicate patterns in weight at age and fecundity at weight observed in the Windermere pike. We optimized the parameters ε_1, ε_2, κ_0, and κ_m in Equations (3) and (5) in the DEB using the optimParallel() package in R (method L-BFGS-B) to fit the model to observed growth and fecundity (Appendix S1: Section S2). Note that the main analysis was based on varying κ_0.

The temperature dependence of maintenance and consumption is a key component of this study, and we based our parameterization of those functions (Equations 3 and 4) on the meta-analysis of respirometry and feeding experiments on fish by Lindmark et al. (2022). Consequently, our temperature dependence of maintenance and consumption were not species specific. Nonetheless, this parameterization in combination with the parameterization described earlier rendered relevant temperature-size-rule (TSR) type growth trajectories (faster growth and development early in life but reduced adult or maximum body sizes) suitable for our study and fitting the observed growth patterns of Windermere pike (size at age Figure 2a, Appendix S1: Section S2).

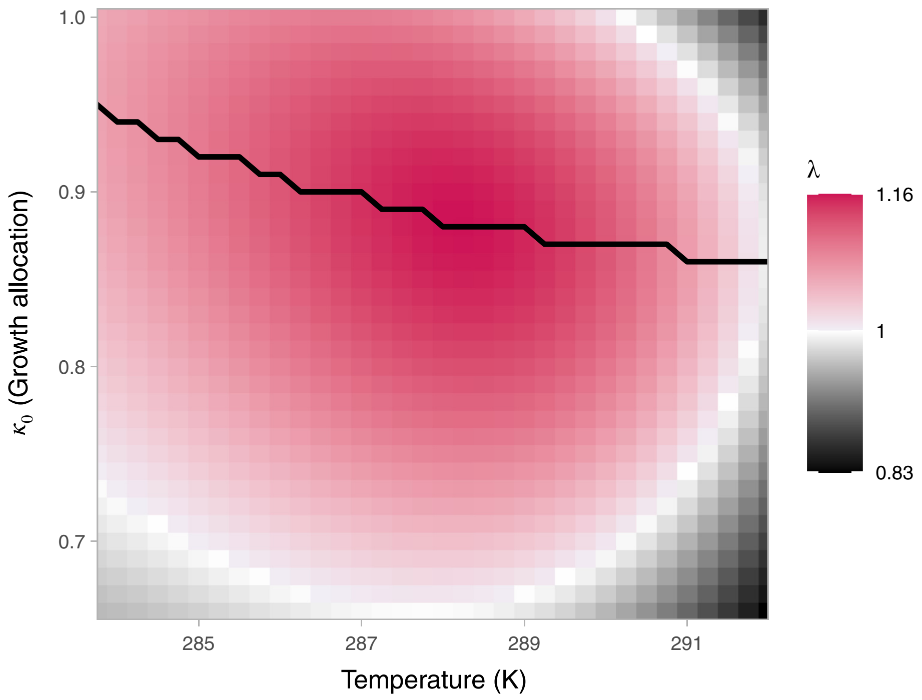

FIGURE 2 Optimal energy allocation to growth (κ_0^*, solid line) predicted from dynamic energy budget integral projection model (DEB–IPM) for Windermere pike. Color indicates the fitness landscape (λ) defined by values of energy allocation (κ_0) and temperature (T).

Analyses

For numerical calculations, we discretize the continuous size distribution in the IPM to a vector of size classes. We then obtain a stage-structured matrix model, with the first stage representing eggs and the other stages representing size class (where the size class bin width, or matrix mesh size, is a parameter adjusted in the numerical analysis of the model). We use the midpoint rule for the numerical approximation of the IPM and select a bin width in our size interval (0–20,000 g) that is small enough for any further increase in the number of size classes to not affect the estimate of λ nor the stable size structure (resulting in 1000 size classes, Appendix S1: Section S4). From this matrix model we calculate the long-term population growth rate (λ) and the stable size distribution using projection (Ellner et al., 2016). Vindenes et al. (2014) estimated the average λ of Windermere pike to 1.04 over the study period, and their analysis indicated an increase of λ with temperature.

We calculate λ from the DEB–IPM in a temperature range of 285–293 K (12–20°C) and a κ_0 range of 0.5–1. This temperature range encompasses mean annual temperatures in Windermere for the period April–August measured between 1940 and 2000 (Winfield & Fletcher, 2013) and possible future increases in mean temperature. For each temperature, we identify the optimal energy allocation as the κ_0 that maximizes fitness (λ) and denote it by κ_0^*.

We use two separate approaches (sensitivity analysis and survival probability contrast) to analyzing how κ_0^* affected fitness at a given temperature. The first is a sensitivity (perturbation) analysis where we decompose the sensitivity $d\lambda/d\kappa_0^*$ (which is approximately 0) to components of each demographic function across size (only age 1 size, growth, and fecundity directly depend on κ_0 via the DEB). We conduct this sensitivity analysis for three temperatures (287, 289, 291 K; see Appendix S1: Section S5 for detailed methods and analytical expressions of the decomposition). The sensitivity contribution from survival is zero because survival does not directly depend on κ_0 in our model and thus only indirectly influences κ_0^*. To investigate how survival affects the optimal energy allocation to growth and reproduction, we therefore test two survival scenarios in addition to the size- and temperature-dependent survival (Figure 4d) used in our main model. The first scenario assumes a temperature-independent survival $a(m_s)$ that corresponds to survival at mean temperature (287 K; Figure 4b), and the second assumes a constant (both size- and temperature-independent) survival that equaled the asymptote at the mean temperature ($a = 0.68$, Figure 4c). This removes the high mortality characterizing early life of pike and many other species and provides a test of how the allocation strategy would change in such a hypothetical life history.

RESULTS

The optimal allocation of energy to somatic growth (κ_0^*), that is, the κ_0 value maximizing mean fitness λ, declines over temperature in our DEB–IPM (Figure 2). Thus, as temperature increases, an individual should allocate more energy to reproduction relative to somatic growth. We find that this pattern is due to an increasing significance of demographic processes in early life for fitness as temperature increases. With warming, somatic growth and survival decrease at large sizes while increasing at small sizes (increased growth means faster escape from high mortality in early life, Figure 3a,c,d). Therefore, allocation to somatic growth plays a critical and temperature-dependent role for λ, which governs the shape of optimal allocation over temperature (Figure 4). Furthermore, fecundity increases for all sizes with warming (Figure 3b), and, in combination with a shift in the size distribution toward smaller and medium-sized individuals (Figure 3f), warming reduces the importance of allocation to somatic growth relative to reproduction for λ (Figure 5).

Emergent effects of size and temperature on demographic functions and population structure

Apart from temperature-dependent survival, the basis for changes in optimal allocation in response to warming is the response of physiological processes in the size- and temperature-dependent DEB model (maintenance and consumption Equations 1–5) that determine the demographic functions and ultimately population size structure in the IPM. At a given temperature, these physiological processes result in decreasing somatic growth and increasing fecundity with size since less energy is available for growth and more for reproduction (Figure 3a,b, Appendix S1: Section S1). The somatic growth rate decreases with size via two mechanisms. First, maintenance costs rise relative to consumption because of the difference in size exponent between the two rates (Table 1). Second, growing fish allocate a larger fraction of available energy to reproductive reserve ($\kappa(m)$ decreases, Equation 5). The individual thus maintains high fecundity at the cost of reduced somatic growth (Figure 3a). Warming leads to further declines in the growth of large individuals (Figure 3a) as maintenance costs increase

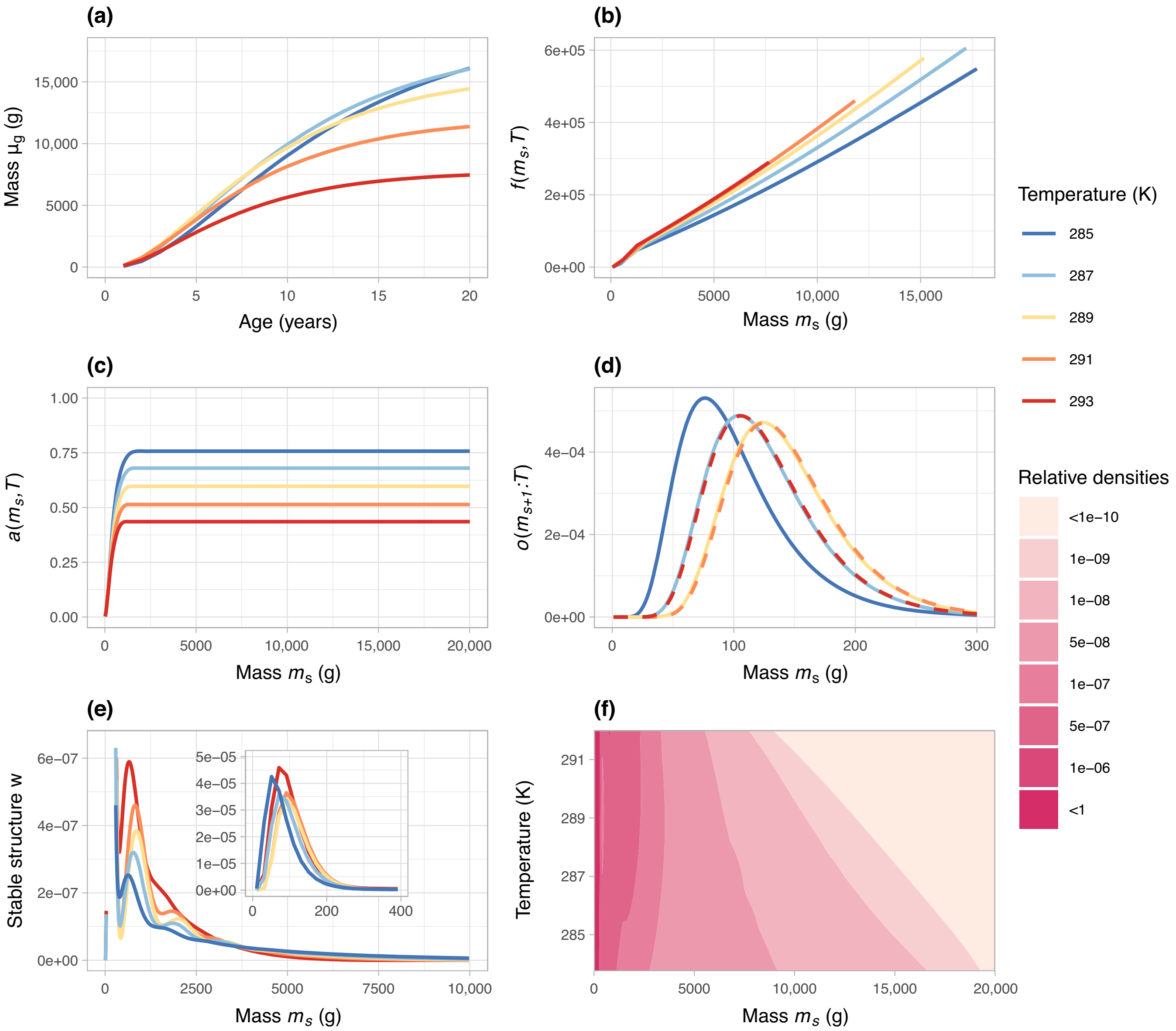

FIGURE 3 Emergent effects of size and temperature on demographic functions (a–d) and (e–f) in dynamic energy budget integral projection model (DEB–IPM) for Windermere pike; mean size at age (a), size-specific fecundity (eggs produced in year $s+1$ by indivduals of size m_s in year s) (b), yearly survival probability (c), size distribution at age 1 (d), and stable size structure (e) (main plot is for age 2 pike and older and inset plot for age 1). All shown for $\kappa_0 = 0.89$ (i.e., 89% of daily assimilated energy for an 0 g individual is allocated to growth and maintenance) and five temperatures between 285 and 293 K. The stable structure surface (f) is a function of temperature and size with bins of relative densities in the stable structure (logarithm of upper boundaries of the bins for visualization purposes).

exponentially while consumption is unimodal over the full temperature range (the optimum temperature for growth thus declines with size, Appendix S1: Section S1). Somatic growth, however, increases with temperature for small individuals, thereby increasing the mean of the size distribution at age 1 (Figure 3d, $T \leq 291$ K). Along with the decreased growth at large size, this causes an individual-level growth trajectory in accordance with the TSR (size at age, Figure 3a). At $T > 291$ K, growth decreases with temperature irrespective of size as the maintenance rate increases in relation to consumption rates (Figure 3a,d). Energy allocated to reproductive reserve increases with temperature because it depends on consumption (Equations 7a–7c), which increases with temperature up to 292 K. Consequently, fecundity at a given body size increases with temperature in the studied temperature range (285–293 K, Figure 3b). That fecundity—for a fixed proportion of energy allocated to reproduction—increases with warming is thus an emergent property of the DEB model.

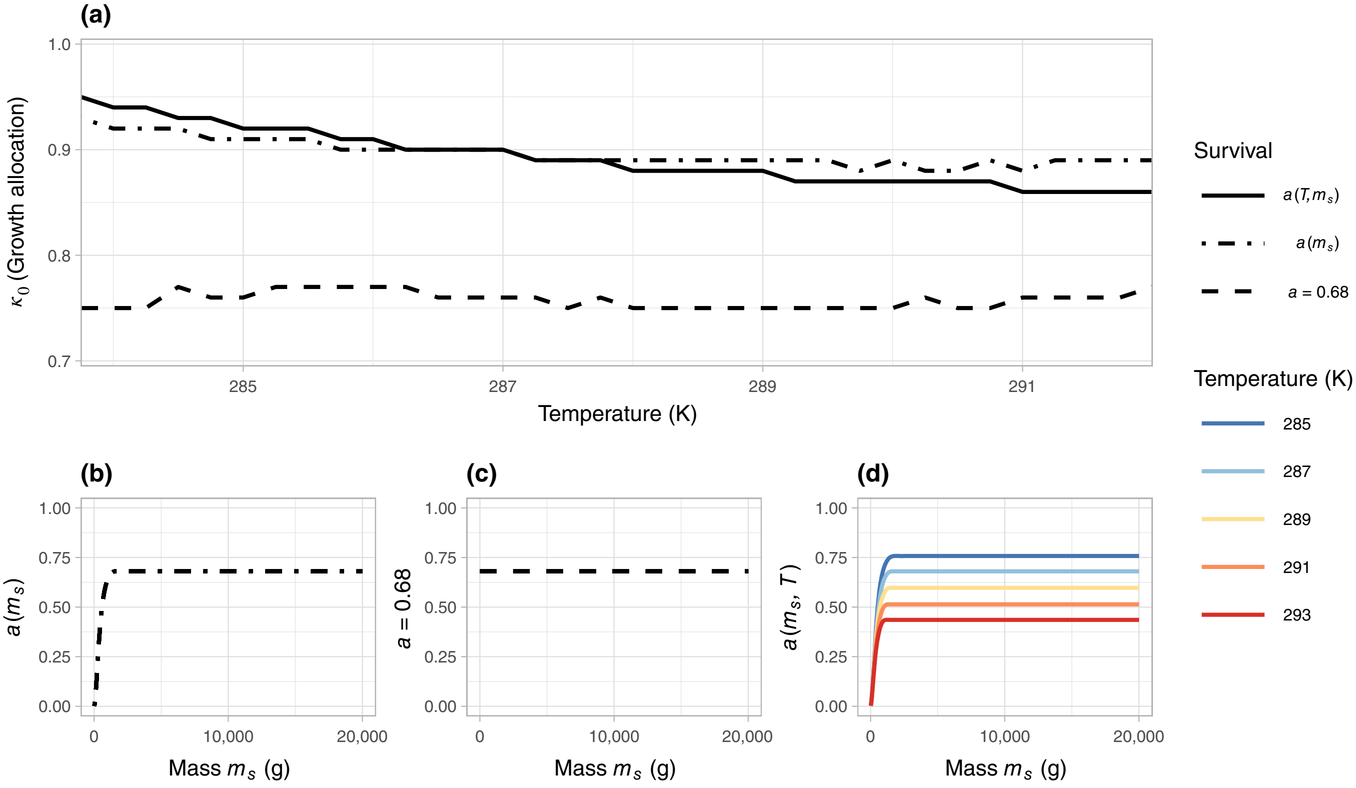

FIGURE 4 Temperature-dependent optimal energy allocation strategy (κ_0^*) for three different survival functions (a), with size and temperature dependence of survival shown in panels (c–e). The solid line is the main model survival, $a(m_s, T)$ (d); as in Figure 2, the dashed-dotted line is the temperature-independent version, $a(m_s)$ (b), of the main model; and the dashed line is constant survival ($a = 0.68$) (c). See Appendix S1: Section S7 for fitness landscapes and stable-size structure surface for the survival contrasts.

The size- and temperature-dependent rates of maintenance and consumption in the DEB and their effects on the demographic functions cause shifts in the population size structure (Figure 3e,f, using constant allocation $\kappa_0 = 0.89$). Independent of temperature, young individuals of small sizes (e.g., age 1–3, peaks in Figure 3e) dominate the population numerically. However, the warming-induced increase in reproductive output and in somatic growth rate and mean size, and thus the survival of small individuals (Figure 3a,c,d), causes high relative densities of small individuals at higher temperatures (Figure 3e,f). At low temperatures, a larger proportion of individuals appears at larger sizes (Figure 3f). The proportion of larger individuals declines with increasing temperature as the somatic growth of those individuals declines, or they die from temperature-induced mortality (Figure 3c). Consequently, warming truncates the size distribution (Figure 3f).

Effects of temperature on optimal energy allocation

We find that the optimal allocation strategy is to allocate a larger proportion of the energy to reproductive reserve at the cost of somatic growth when temperature increases, that is, higher κ_0^* at low ($\kappa_0^* > 0.9$, $T < 287$ K) compared to high temperatures ($\kappa_0^* < 0.9$, $T > 287$ K, Figure 2). Note that $\kappa(m)$ (Equation 5) declines with size and that $\kappa_0 = 1$ means that all energy is allocated to growth for $m = 0$. We show optimal size at age and fecundity in Appendix S1: Section S6.

Our sensitivity (perturbation) analyses performed at different temperatures demonstrate the size dependence of the trade-off in allocation between growth and reproduction (the sum of contributions to the sensitivity from growth and age 1 size is positive, but it is negative for fecundity; Figure 5). The demographic processes of small individuals have a higher impact on how the energy allocation affects fitness, which increases with temperature. This is particularly evident for the sensitivity contributions from size at age 1 and fecundity (Figure 5), whereas the contributions via growth remain relatively high also for individuals < 5000 g. The warming-induced loss of larger individuals and increase of small individuals (Figure 3e,f), evidenced by their respective relative decrease and increase in sensitivity contribution at higher temperatures, reduces the importance of allocation to growth (age > 1) to maintain high fitness (Figure 5, $T = 289, 291$ K). The relative

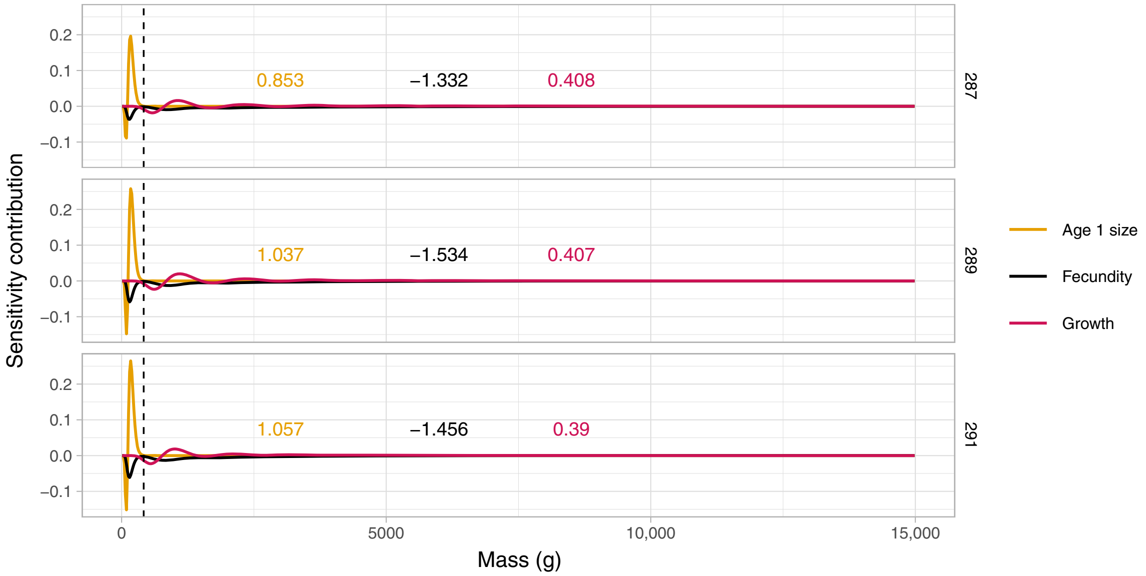

FIGURE 5 Relative contribution of size at age 1 (yellow), fecundity (black), and growth (purple) across size to sensitivity of fitness (λ) to κ_0, measured at optimal energy allocation κ_0^* at three temperatures ($\kappa^*_{0,T=287} = 0.9$, $\kappa^*_{0,T=289} = 0.88$, $\kappa^*_{0,T=291} = 0.86$). The numbers in each panel correspond to the sum of sensitivity contributions from each demographic function.

importance of energy allocation for fecundity and size at age 1 for fitness thus increases in comparison to growth (note that λ differs between temperatures and that comparisons therefore should be made regarding the relative contributions within each temperature). In warmer environments, slight changes in energy allocation will thus have relatively larger effects on fitness through the growth early in life (here size at age 1) and fecundity of small and newly matured, rather than via the growth and fecundity of larger individuals.

Because survival acts only indirectly on energy allocation, we used a different approach to study the role of the size-dependent survival on energy allocation strategies. Here, we contrasted the main model for survival (Figure 3c) with two alternative survival models: temperature-independent survival (where the asymptote for weight is constant over a temperature range) and size- and temperature-independent survival (Figure 4b,c). The latter is much higher for small individuals compared to the main model and removes the effects of growth on survival so that the only fitness benefit of growth is increased fecundity. This has significant fitness consequences and produces high λ values (see Appendix S1: Section S7 for the modeled fitness landscapes and stable size structure surface using the alternative survival probabilities). Importantly, this size- and temperature-independent survival probability generates a pronounced contrast in how the optimal energy allocation varies with temperature: κ_0^* changes less with temperature and is much lower ($0.7 < \kappa_0 < 0.77$) compared to the main model ($0.86 \leq \kappa_0 \leq 95$, Figure 4a). In combination with the sensitivity analysis of the main model (Figure 5), this confirms that the survival of small individuals, being highly affected by early growth, is an important driver of optimal energy allocation.

Contrasting the main, temperature-dependent survival model, $a(x, T)$, with a temperature-independent, $a(x)$, survival asymptote (Figure 4c) yields the same qualitative result but a smaller decrease in κ_0^* with increasing temperature (Figure 4a). Temperature-independent survival thus leads to a higher allocation to somatic growth at high temperatures compared to temperature-dependent survival (Figure 4b). Consequently, increased allocation to reproductive reserve at high temperatures partly occurs because warming decreases the survival of large individuals.

DISCUSSION

In this study, we demonstrate how temperature effects on metabolism and consumption, via emergent temperature-sensitive size dependencies of individual growth, fecundity, and survival (via growth), affect population size structure and fitness. The individual- and population-level responses to warming predicted from our DEB–IPM for Windermere pike represent common (but not universal) patterns of intraspecific changes in the body size of natural ectothermic populations (Audzijonyte et al., 2020; van Dorst et al., 2018; van Rijn et al., 2017). We show that increases in energy allocation to reproduction relative to somatic growth can optimize mean fitness in a warmer climate, depending on the joint effects of demographic processes on fitness. Two main size-dependent demographic responses to warming explain the change in the optimal energy allocation: The first and most vital response is that affecting the trade-off between early growth that improves survival early in life and the reproductive output of small (and abundant) individuals. This trade-off is shaped by the warming-induced increases in fecundity and somatic growth of small individuals (Figure 3) and subsequent increases in early survival with growth, making energy allocation to reproduction increasingly important for population growth as temperature increases (Figures 2 and 5). The second process is the somatic growth, survival, and, thus, potential reproductive output of larger individuals. Here, warming decreases the survival of individuals >1000 g (Figure 3c) and reduces the growth of large individuals (Figure 3a), reducing their relative abundance and, thus, the fitness benefits of allocation to somatic growth for future reproductive output. As previously suggested, warming should, hence, favor allocation to reproductive reserve (Audzijonyte et al., 2018; Fryxell et al., 2020; Kozlowski et al., 2004). The combination of the direct effects of temperature in our model (i.e., the TSR emerging from temperature-dependent maintenance and consumption, and temperature-dependent survival), and the resulting changes in optimal energy allocation suggest a shift toward smaller but more fecund individuals in warming environments, given that the population can evolve toward this optimum strategy.

The indirect effects of growth on survival plays a key role in determining the warming-induced increase in allocation to reproduction in our model. A high allocation to somatic growth facilitates fast growth early in life, when mortality is typically high, at the cost of fecundity (Pepin, 1991; Post & Parkinson, 2001; Roff et al., 2006). By the same principle, high juvenile growth rates due to increases in temperature can result in plastic increases in allocation to reproduction (Ward et al., 2017), which then decreases temperature-adjusted growth rates, that is, countergradient variation in growth (Conover & Present, 1990; Fryxell et al., 2020). In our baseline model, the survival of individuals <1000 g increases with body size, and early somatic growth increases with temperature. In combination with warming-induced increases in fecundity, this reduces the costs of early reproduction. Accordingly, our analysis of survival probability makes it clear that both a generally higher allocation to somatic growth and the qualitative change in optimal allocation (decreasing κ_0^*) with warming depend on temperature effects on survival. Here, it is important to consider additional temperature-dependent factors that we did not account for and that may affect age- or body size–specific allocation. These include temperature effects on survival in the first year of life and the fact that development rate may affect size at maturation (Atkinson, 1994; Kozlowski et al., 2004; Kuparinen et al., 2011). Furthermore, temperature-dependent increases in the growth rate and survival of small individuals rely on food availability being sufficient to meet warming-induced increases in maximum consumption rate (Huey & Kingsolver, 2019; Lemoine, 2019; Myrvold & Kennedy, 2015). If food is not available at sufficient levels, there will be no fitness benefits of increased allocation to reproduction. Consequently, understanding how warming affects energy allocation requires knowledge of not only the consumption–maintenance balance but also their interplay with temperature-dependent survival early in life.

We show that warming-induced reduction in the somatic growth and survival of large individuals amplifies the fitness benefits of increased allocation to reproduction. A potential decrease in survival at larger sizes (or older age), for example from harvesting, would reduce the potential for future (and implicitly larger) reproductive output and reduce the fitness benefit of growth (Kozlowski, 1997; Perrin & Sibly, 1993). This benefit is already reduced in our model because warming decreases both the survival probability and growth rate of large individuals, in turn reducing their abundance and contribution to mean fitness (λ) via reproduction. We assume that as an individual grows, energy allocation to reproductive reserve would be increasingly prioritized over somatic growth (Equation 5). As a result of this, our model generated a mass–fecundity relationship that fit well what we observe in our model population (the Windermere pike, Appendix S1: Section S2) and, generally, with observations of high reproductive output of large females (in fishes: Barneche et al., 2018, in insects: Honěk, 1993). This energy allocation strategy implies that the present energy allocation to growth increases future reproductive output and maximizes growth and survival for small individuals and reproduction for large individuals (Kozlowski, 1997). Via changes in growth and survival, warming can directly reduce those positive relationships between size and fecundity (Arendt, 2015). Increases in reproductive effort of small individuals, in response to ancestral exposure to warming, as shown by Loisel et al. (2019) or by evolutionary adaptation as shown by Fryxell et al. (2020), remediate such negative effects. These studies thus support our findings. However, we did not quantify the importance of the slope between energy allocation (but used it to fit the model to data) and size for optimal energy allocation in a warmer climate, which represents an area of future research. Maternal size and temperature may also affect trade-offs between offspring number and quality (e.g., more nutrients provided per egg), with potential effects on survival and growth in the first year (Alix et al., 2020; Lukšienė et al., 2000; Parratt et al., 2021; Vindenes et al., 2016), and the size-dependent cost of reproduction (Audzijonyte & Richards, 2018) relative to growth. Both examples could affect optimal energy allocation. The temperature-dependent DEB–IPM framework that we have developed is a suitable tool for exploring such relationships in future studies since it builds on a mechanistic description of size- and temperature-dependent energy gain and expenditure.

The TSR type modeled size at age stems from the size and temperature dependence of maintenance and consumption rates, leading to a decline in optimum temperature for growth with body size (Lindmark et al., 2022). In our model, the parameterization of consumption rates and change in allocation with size, $\kappa(m)$, to fit data of growth and reproduction in Windermere pike likely affects this emergent TSR. Recent warming experiments on reproduction and metabolism in zebrafish suggest that TSR and declining body sizes are caused by increased allocation to gonadal tissue at high temperatures (Wootton et al., 2022). Over six generations in the lab, acclimation to higher temperatures resulted in lowered metabolism of adults, increases in growth rates of smaller fish, and increased allocation to reproduction. Similar observations have been made in the wild, with increasing growth rates of small individuals in warmer environments found across multiple generations (Huss et al., 2019). Interestingly, our results suggest that the increase in consumption in relation to metabolism induced by warming should lead to increasing allocation to reproductive reserve. This is in line with the results found by Wootton et al. (2022), but the mechanism behind our findings does not rely on the acclimation of metabolic rates yet represents the same effects. Importantly, we think our framework adheres to Wootton et al.'s (2022) call for the use of better growth models that include reproductive allocation.

Our method is novel because the DEB–IPM accounts for the causal relationships between intraspecific interdependencies of body-size and temperature effects on consumption and metabolism, as well as on emergent individual- and population-level effects. Because of this, we could analyze changes in optimal allocation with temperature and reveal how trade-offs among demographic processes at different sizes govern optimal allocation. Ecological and demographic analyses of IPMs have long enabled analysis of how size-structured demographic rates affect evolutionary processes (Easterling et al., 2000; Rees & Rose, 2002; Vindenes et al., 2016). However, the temperature dependence of vital rates in IPMs has, to our knowledge, been fitted to observed patterns of demographic rates (Vindenes et al., 2014) rather than being modeled as the emergent properties of temperature- and size-dependent bioenergetics, as we did in this study. Smallegange et al. (2017) combined the DEB framework (Kooijman, 1993) with IPMs to enable similar mechanistic links between individual growth and fecundity and environmental conditions in a DEB–IPM. Their approach differs from ours in that it relies on solving the integration of the differential equation for growth rate analytically to estimate von Bertalanffy growth equation parameters. This enables mathematically convenient analytical integration by assuming proportional scaling of maintenance rate with mass and mass scaling proportional to the cube of length (Essington et al., 2001; Kooijman & Metz, 1984; Smallegange et al., 2017). These assumptions are, however, not compatible with the fact that maintenance rate scales with both temperature and mass, generating functions without closed form and, thus, without analytical solutions. Furthermore, the von Bertalanffy growth model is a largely phenomenological description of growth, unable to incorporate the consequences for reproductive allocation (Czarnoleski & Kozlowski, 1998). At a small computational cost, our numerical approach instead emphasizes the physiologically relevant links between temperature and mass, energetic costs and gains, and allometric reproductive scaling that sets the temperature- and mass-dependent energy budget. Those links provide a transparent physiological underpinning of how warming affects the energy allocation strategies that maximize population growth in the IPM.

Our parameterization and model of temperature effects on the energy budget carry two important assumptions that have implications for analyses of fitness and for optimal energy allocation in response to warming. First, we assumed that optimal allocation of energy to growth versus reproduction was the κ-value $\left(\kappa_0^*\right)$ that maximized mean fitness (λ), which was only possible to calculate for a density-independent model. Our model therefore does not account for density dependence (e.g., via competition for food), which, as for species interactions in general, is affected by warming (Gårdmark & Huss, 2020). Second, our parameterization of the energy budget is mainly based on within-generation effects on metabolism and consumption (and ad libitum feeding experiments). Real-life conditions paint a more complex picture of the developmental and transgenerational effects of warming on, for example, metabolism, affecting the temperature dependence of growth trajectories and allocation strategies (Loisel et al., 2019; Sandblom et al., 2016; Wootton et al., 2022). Such long-term changes in metabolism could also interact with the heritability of allocation (our model represents the mean allocation strategy) since selection on genotypes representing different life-history (e.g., allocation) trade-offs may depend on metabolic phenotypes and their energy acquisition, that is, genotype-by-environment variation (King et al., 2011; but see Prokkola et al., 2022). Evolutionary assessments not constrained by these two assumptions require specificity (e.g., of species interactions in the first, or heritability of traits in the second case), whereas our study focuses on the general effects of warming on optimal energy allocation.

To conclude, the demographic effects of warming explain the increased allocation to reproduction because warming increases selection through, or the dependence on, demographic processes early in life for population growth (Durant & Hjermann, 2017; Vindenes et al., 2016). A high allocation of energy to reproduction, smaller maximum body size, and shorter generation time makes a population increasingly dependent on reproduction, resulting in increased variation in population size (Hidalgo et al., 2011; Ohlberger et al., 2014; Röpke et al., 2021). Our results suggest that through these effects populations can become more sensitive to fluctuating environmental conditions, with less predictable dynamics, leading to more difficult management.

AUTHOR CONTRIBUTIONS

All authors contributed to the study's conception. With input from all authors, Viktor Thunell and Anna Gårdmark conceptualized the dynamic energy budget model, and Yngvild Vindenes and Viktor Thunell conceived the integral projection model. Viktor Thunell developed the model with the help of Yngvild Vindenes and performed the analysis. Yngvild Vindenes derived the analytical expressions for the sensitivity of the IPM. Viktor Thunell led the writing, and all authors contributed to the revision of the manuscript.

ACKNOWLEDGMENTS

We thank Max Lindmark for fruitful discussions and for sharing preliminary results on size–temperature scaling of metabolic and consumption rates and Elizabeth Duskey for building the optimization code for parameter estimation. We thank all field and lab workers, past and present, for their contributions to long-term research on Windermere, now supported by the Natural Environment Research Council, Award NE/R016429/1, as part of the UK-SCAPE program delivering National Capability. This study was supported by grants from the Research Council of Norway (project ECOVAR; Grant 244404 to Yngvild Vindenes) and the Swedish Research Council (Grant 2015-03752 to Anna Gårdmark).

CONFLICT OF INTEREST

The authors declares no conflict of interest.

DATA AVAILABILITY STATEMENT

Data on growth (Winfield et al., 2013b) and fecundity (Winfield et al., 2013a) of the Windermere Northern pike are available in the NERC Environmental Information Data Centre at https://doi.org/10.5285/637d60d6-1571-49af-93f7-24c1279d884d and https://doi.org/10.5285/b8886915-14cb-44df-86fa-7ab718acf49a, respectively. Windermere Lake temperature data (Winfield & Fletcher, 2013) are available in the NERC Environmental Information Data Centre at https://doi.org/10.5285/9520664c-eb4d-4700-b064-5d215d23e595. All R code (Thunell et al., 2022) used to build the model and generate the output, results and corresponding figures is available in Zenodo at https://doi.org/10.5281/zenodo.7391013.

ORCID

Viktor Thunell https://orcid.org/0000-0003-1383-6387
Anna Gårdmark https://orcid.org/0000-0003-1803-0622
Magnus Huss https://orcid.org/0000-0002-5131-6000
Yngvild Vindenes https://orcid.org/0000-0003-1197-5818

REFERENCES

Ahti, P. A., A. Kuparinen, and S. Uusi-Heikkilä. 2020. "Size Does Matter — The Eco-Evolutionary Effects of Changing Body Size in Fish." *Environmental Reviews* 28(3): 311–24. https://doi.org/10.1139/er-2019-0076.

Alix, M., O. S. Kjesbu, and K. C. Anderson. 2020. "From Gametogenesis to Spawning: How Climate-Driven Warming Affects Teleost Reproductive Biology." *Journal of Fish Biology* 97(3): 607–32. https://doi.org/10.1111/jfb.14439.

Arendt, J. 2015. "Why Get Big in the Cold? Size-Fecundity Relationships Explain the Temperature-Size Rule in a Pulmonate Snail (Physa)." *Journal of Evolutionary Biology* 28(1): 169–78. https://doi.org/10.1111/jeb.12554.

Armstrong, J. D., I. G. Priede, and M. C. Lucas. 1992. "The Link between Respiratory Capacity and Changing Metabolic Demands during Growth of Northern Pike, *Esox lucius* L." *Journal of Fish Biology* 41(sB): 65–75. https://doi.org/10.1111/j.1095-8649.1992.tb03869.x.

Atkinson, D. 1994. "Temperature and Organism Size—A Biological Law for Ectotherms?" In *Advances in Ecological Research*, edited by M. Begon and A. H. Fitter, Vol. 25, 1–58. Cambridge, MA: Academic Press.

Audzijonyte, A., and S. A. Richards. 2018. "The Energetic Cost of Reproduction and Its Effect on Optimal Life-History Strategies." *The American Naturalist* 192(4): E150–62. https://doi.org/10.1086/698655.

Audzijonyte, A., S. A. Richards, R. D. Stuart-Smith, G. Pecl, G. J. Edgar, N. S. Barrett, N. Payne, and J. L. Blanchard. 2020. "Fish Body Sizes Change with Temperature but Not all Species Shrink with Warming." *Nature Ecology and Evolution* 4(6): 809–14. https://doi.org/10.1038/s41559-020-1171-0.

Audzijonyte, A., D. R. Barneche, A. R. Baudron, J. Belmaker, T. D. Clark, C. Tara Marshall, J. R. Morrongiello, I. van Rijn, and A. Bates. 2018. "Is Oxygen Limitation in Warming Waters a

Valid Mechanism to Explain Decreased Body Sizes in Aquatic Ectotherms?" *Global Ecology and Biogeography* 28(2): 64–77. https://doi.org/10.1111/geb.12847.

Barneche, D. R., D. R. Robertson, C. R. White, and D. J. Marshall. 2018. "Fish Reproductive-Energy Output Increases Disproportionately with Body Size." *Science* 360(6389): 642–5. https://doi.org/10.1126/science.aao6868.

Baudron, A. R., C. L. Needle, A. D. Rijnsdorp, and C. T. Marshall. 2014. "Warming Temperatures and Smaller Body Sizes: Synchronous Changes in Growth of North Sea Fishes." *Global Change Biology* 20(4): 1023–31. https://doi.org/10.1111/gcb.12514.

Byström, P., J. Andersson, A. Kiessling, and L.-O. Eriksson. 2006. "Size and Temperature Dependent Foraging Capacities and Metabolism: Consequences for Winter Starvation Mortality in Fish." *Oikos* 115(1): 43–52. https://doi.org/10.1111/j.2006.0030-1299.15014.x.

Byström, P., L. Persson, and E. Wahlström. 1998. "Competing Predators and Prey: Juvenile Bottlenecks in Whole-Lake Experiments." *Ecology* 79(6): 2153–67. https://doi.org/10.1890/0012-9658(1998)079[2153:Cpapjb]2.0.Co;2.

Christensen, E. A. F., M. B. S. Svendsen, and J. F. Steffensen. 2020. "The Combined Effect of Body Size and Temperature on Oxygen Consumption Rates and the Size-Dependency of Preferred Temperature in European Perch *Perca fluviatilis*." *Journal of Fish Biology* 97: 794–803. https://doi.org/10.1111/jfb.14435.

Clarke, A., and K. P. P. Fraser. 2004. "Why Does Metabolism Scale with Temperature?" *Functional Ecology* 18(2): 243–51. https://doi.org/10.1111/j.0269-8463.2004.00841.x.

Conover, D. O., and T. M. Present. 1990. "Countergradient Variation in Growth Rate: Compensation for Length of the Growing Season among Atlantic Silversides from Different Latitudes." *Oecologia* 83(3): 316–24. https://doi.org/10.1007/BF00317554.

Corriero, A., R. Zupa, C. C. Mylonas, and L. Passantino. 2021. "Atresia of Ovarian Follicles in Fishes, and Implications and Uses in Aquaculture and Fisheries." *Journal of Fish Diseases* 44(9): 1271–91. https://doi.org/10.1111/jfd.13469.

Czarnoleski, M., and J. Kozlowski. 1998. "Do Bertalanffy's Growth Curves Result from Optimal Resource Allocation?" *Ecology Letters* 1(1): 5–7. https://doi.org/10.1046/j.1461-0248.1998.0007b.x.

Daufresne, M., K. Lengfellner, and U. Sommer. 2009. "Global Warming Benefits the Small in Aquatic Ecosystems." *Proceedings of the National Academy of Sciences of the United States of America* 106(31): 12788–93. https://doi.org/10.1073/pnas.0902080106.

Diana, J. S. 1983. "An energy budget for northern pike (*Esox lucius*)." *Canadian Journal of Zoology* 61(9): 1968–75. https://doi.org/10.1139/z83-259.

Durant, J. M., and D. Ø. Hjermann. 2017. "Age-Structure, Harvesting and Climate Effects on Population Growth of Arcto-Boreal Fish Stocks." *Marine Ecology Progress Series* 577: 177–88. https://doi.org/10.3354/meps12210.

Easterling, M. R., S. P. Ellner, and P. M. Dixon. 2000. "Size-Specific Sensitivity: Applying a New Structured Population Model." *Ecology* 81(3): 694–708. https://doi.org/10.1890/0012-9658(2000)081[0694:Sssaan]2.0.Co;2.

Ellner, S. P., D. Z. Childs, and M. Rees. 2016. *Data-Driven Modelling of Structured Populations, Lecture Notes on Mathematical Modelling in the Life Sciences*. Cham: Springer International Publishing.

Englund, G., G. Öhlund, C. L. Hein, and S. Diehl. 2011. "Temperature Dependence of the Functional Response." *Ecology Letters* 14(9): 914–21. https://doi.org/10.1111/j.1461-0248.2011.01661.x.

Essington, T. E., J. F. Kitchell, and C. J. Walters. 2001. "The von Bertalanffy Growth Function, Bioenergetics, and the Consumption Rates of Fish." *Canadian Journal of Fisheries and Aquatic Sciences* 58(11): 2129–38. https://doi.org/10.1139/f01-151.

Forster, J., and A. G. Hirst. 2012. "The Temperature-Size Rule Emerges from Ontogenetic Differences between Growth and Development Rates." *Functional Ecology* 26(2): 483–92. https://doi.org/10.1111/j.1365-2435.2011.01958.x.

Frost, W. E., and C. Kipling. 1967. "A Study of Reproduction, Early Life, Weight-Length Relationship and Growth of Pike, *Esox lucius* L., in Windermere." *The Journal of Animal Ecology* 36: 3. https://doi.org/10.2307/2820.

Fryxell, D. C., A. N. Hoover, D. A. Alvarez, F. J. Arnesen, J. N. Benavente, E. R. Moffett, M. T. Kinnison, K. S. Simon, and E. P. Palkovacs. 2020. "Recent Warming Reduces the Reproductive Advantage of Large Size and Contributes to Evolutionary Downsizing in Nature." *Proceedings of the Biological Sciences* 287(1928): 20200608. https://doi.org/10.1098/rspb.2020.0608.

Gårdmark, A., and M. Huss. 2020. "Individual Variation and Interactions Explain Food Web Responses to Global Warming." *Philosophical Transactions of the Royal Society of London. Series B, Biological Sciences* 375(1814): 20190449. https://doi.org/10.1098/rstb.2019.0449.

Gillooly, J. F., J. H. Brown, G. B. West, V. M. Savage, and E. L. Charnov. 2001. "Effects of Size and Temperature on Metabolic Rate." *Science* 293(5538): 2248–51. https://doi.org/10.1126/science.1061967.

Gunderson, D. R. 1997. "Trade-off between Reproductive Effort and Adult Survival in Oviparous and Viviparous Fishes." *Canadian Journal of Fisheries and Aquatic Sciences* 54(5): 990–8. https://doi.org/10.1139/f97-019.

Heino, M., and V. Kaitala. 2001. "Evolution of Resource Allocation between Growth and Reproduction in Animals with Indeterminate Growth." *Journal of Evolutionary Biology* 12(3): 423–9. https://doi.org/10.1046/j.1420-9101.1999.00044.x.

Hidalgo, M., T. Rouyer, J. C. Molinero, E. Massutí, J. Moranta, B. Guijarro, and N. C. Stenseth. 2011. "Synergistic Effects of Fishing-Induced Demographic Changes and Climate Variation on Fish Population Dynamics." *Marine Ecology Progress Series* 426: 1–12. https://doi.org/10.3354/meps09077.

Honěk, A. 1993. "Intraspecific Variation in Body Size and Fecundity in Insects: A General Relationship." *Oikos* 66(3): 483. https://doi.org/10.2307/3544943.

Huey, R. B., and J. G. Kingsolver. 2019. "Climate Warming, Resource Availability, and the Metabolic Meltdown of Ectotherms." *The American Naturalist* 194(6): E140–50. https://doi.org/10.1086/705679.

Hultin, E. 1955. "The Influence of Temperature on the Rate of Enzymic Processes." *Acta Chemica Scandinavica* 9(170): 1700–10.

Huss, M., M. Lindmark, P. Jacobson, R. M. van Dorst, and A. Gårdmark. 2019. "Experimental Evidence of Gradual Size-Dependent Shifts in Body Size and Growth of Fish in Response to Warming." *Global Change Biology* 25(7): 2285–95. https://doi.org/10.1111/gcb.14637.

Ikpewe, I. E., A. R. Baudron, A. Ponchon, P. G. Fernandes, and R. Pinto. 2020. "Bigger Juveniles and Smaller Adults: Changes in Fish Size Correlate with Warming Seas." *Journal of Applied Ecology* 58(4): 847–56. https://doi.org/10.1111/1365-2664.13807.

King, E. G., D. A. Roff, and D. J. Fairbairn. 2011. "The Evolutionary Genetics of Acquisition and Allocation in the Wing Dimorphic Cricket, *Gryllus firmus*." *Evolution* 65(8): 2273–85. https://doi.org/10.1111/j.1558-5646.2011.01296.x.

Kipling, C., and W. E. Frost. 1970. "A Study of the Mortality, Population Numbers, Year Class Strengths, Production and Food Consumption of Pike, *Esox lucius* L., in Windermere from 1944 to 1962." *The Journal of Animal Ecology* 39(1): 115. https://doi.org/10.2307/2892.

Koenigstein, S., F. C. Mark, S. Gößling-Reisemann, H. Reuter, and H.-O. Poertner. 2016. "Modelling Climate Change Impacts on Marine Fish Populations: Process-Based Integration of Ocean Warming, Acidification and Other Environmental Drivers." *Fish and Fisheries* 17(4): 972–1004. https://doi.org/10.1111/faf.12155.

Kooijman, S. A. L. M. 1993. *Dynamic Energy Budgets in Biological Systems Theory and Applications in Ecotoxicology*. Cambridge: Cambridge University Press.

Kooijman, S. A. L. M., and J. Metz. 1984. "On the Dynamics of Chemically Stressed Poplations." *Ecotoxicology and Environmental Safety* 8: 254–74.

Kozlowski, J. 1997. "Optimal Allocation of Resources Explains Interspecific Life-History Patterns in Animals with Indeterminate Growth." *Proceedings of the Royal Society B: Biological Sciences* 263(1370): 559–66. https://doi.org/10.1098/rspb.1996.0084.

Kozlowski, J., M. Czarnoleski, and M. Danko. 2004. "Can Optimal Resource Allocation Models Explain why Ectotherms Grow Larger in Cold?" *Integrative and Comparative Biology* 44(6): 480–93. https://doi.org/10.1093/icb/44.6.480.

Kuparinen, A., J. M. Cano, J. Loehr, G. Herczeg, A. Gonda, and J. Merilä. 2011. "Fish Age at Maturation Is Influenced by Temperature Independently of Growth." *Oecologia* 167(2): 435–43. https://doi.org/10.1007/s00442-011-1989-x.

Law, R. 1979. "Optimal Life Histories Predation." *American Naturalist* 114(3): 399–417.

Le Cren, D. 2001. "The Windermere Perch and Pike Project: An Historical Review." *Freshwater Forum* 15: 3–34.

Lemoine, N. P. 2019. "Considering the Effects of Temperature × Nutrient Interactions on the Thermal Response Curve of Carrying Capacity." *Ecology* 100(4): e02599. https://doi.org/10.1002/ecy.2599.

Lindmark, M., J. Ohlberger, and A. Gårdmark. 2022. "Optimum Growth Temperature Declines with Body Size within Fish Species." *Global Change Biology* 28(7): 2259–71. https://doi.org/10.1111/gcb.16067.

Lindmark, M., J. Ohlberger, M. Huss, and A. Gårdmark. 2019. "Size-Based Ecological Interactions Drive Food Web Responses to Climate Warming." *Ecology Letters* 22(5): 778–86. https://doi.org/10.1111/ele.13235.

Loisel, A., A. Isla, and M. Daufresne. 2019. "Variation of Thermal Plasticity in Growth and Reproduction Patterns: Importance of Ancestral and Developmental Temperatures." *Journal of Thermal Biology* 84: 460–8. https://doi.org/10.1016/j.jtherbio.2019.07.029.

Lukšienė, D., O. Sandström, L. Lounasheimo, and J. Andersson. 2000. "The Effects of Thermal Effluent Exposure on the Gametogenesis of Female Fish." *Journal of Fish Biology* 56(1): 37–50. https://doi.org/10.1111/j.1095-8649.2000.tb02085.x.

Marshall, D. J., and C. R. White. 2019. "Have We Outgrown the Existing Models of Growth?" *Trends in Ecology & Evolution* 34(2): 102–11. https://doi.org/10.1016/j.tree.2018.10.005.

Myrvold, K. M., and B. P. Kennedy. 2015. "Interactions between Body Mass and Water Temperature Cause Energetic Bottlenecks in Juvenile Steelhead." *Ecology of Freshwater Fish* 24(3): 373–83. https://doi.org/10.1111/eff.12151.

Ohlberger, J., E. Edeline, L. A. Vøllestad, N. C. Stenseth, and D. Claessen. 2011. "Temperature-Driven Regime Shifts in the Dynamics of Size-Structured Populations." *The American Naturalist* 177(2): 211–23. https://doi.org/10.1086/657925.

Ohlberger, J., S. J. Thackeray, I. J. Winfield, S. C. Maberly, and L. A. Vøllestad. 2014. "When Phenology Matters: Age-Size Truncation Alters Population Response to Trophic Mismatch." *Proceedings of the Biological Sciences* 281(1793): 20140938. https://doi.org/10.1098/rspb.2014.0938.

Padfield, D., M. Castledine, and A. Buckling. 2020. "Temperature-Dependent Changes to Host-Parasite Interactions Alter the Thermal Performance of a Bacterial Host." *The ISME Journal* 14(2): 389–98. https://doi.org/10.1038/s41396-019-0526-5.

Parratt, S. R., B. S. Walsh, S. Metelmann, N. White, A. Manser, A. J. Bretman, A. A. Hoffmann, R. R. Snook, and T. A. R. Price. 2021. "Temperatures that Sterilize Males Better Match Global Species Distributions than Lethal Temperatures." *Nature Climate Change* 11(6): 481–4. https://doi.org/10.1038/s41558-021-01047-0.

Pepin, P. 1991. "Effect of Temperature and Size on Development, Mortality, and Survival Rates of the Pelagic Early Life History Stages of Marine Fish." *Canadian Journal of Fisheries and Aquatic Sciences* 48(3): 503–18. https://doi.org/10.1139/f91-065.

Perrin, N., and R. M. Sibly. 1993. "Dynamic Models of Energy Allocation and Investment." *Annual Review of Ecology and Systematics* 24(1): 379–410. https://doi.org/10.1146/annurev.es.24.110193.002115.

Post, J. R., and E. A. Parkinson. 2001. "Energy Allocation Strategy in Young Fish: Allometry and Survival." *Ecology* 82(4): 1040–51. https://doi.org/10.1890/0012-9658(2001)082[1040:Easiyf]2.0.Co;2.

Potter, T., and A. Felmy. 2022. "An Ecological Explanation for Hyperallometric Scaling of Reproduction." *Functional Ecology* 36(6): 1513–23. https://doi.org/10.1111/1365-2435.14045.

Prokkola, J. M., E. R. Åsheim, S. Morozov, P. Bangura, J. Erkinaro, A. Ruokolainen, C. R. Primmer, and T. Aykanat. 2022. "Genetic Coupling of Life-History and Aerobic Performance in Atlantic Salmon." *Proceedings of the Biological Sciences* 289(1967): 20212500. https://doi.org/10.1098/rspb.2021.2500.

R Core Team. 2020. *R: A Language and Environment for Statistical Computing*. Vienna: R Foundation for Statistical Computing.

Rees, M., D. Z. Childs, and S. P. Ellner. 2014. "Building Integral Projection Models: A User's Guide." *The Journal of Animal Ecology* 83(3): 528–45. https://doi.org/10.1111/1365-2656.12178.

Rees, M., and K. E. Rose. 2002. "Evolution of Flowering Strategies in Oenothera Glazioviana: An Integral Projection Model Approach." *Proceedings of the Royal Society B: Biological Sciences* 269: 1509–15. https://doi.org/10.1098/rspb.2002.2037.

Roff, D. A., E. Heibo, and L. A. Vøllestad. 2006. "The Importance of Growth and Mortality Costs in the Evolution of the Optimal Life History." *Journal of Evolutionary Biology* 19(6): 1920–30. https://doi.org/10.1111/j.1420-9101.2006.01155.x.

Röpke, C., T. H. S. Pires, J. Zuanon, C. E. C. Freitas, M. C. Hernandes, F. Souza, and S. Amadio. 2021. "Growth–Reproduction Trade-off and Fecundity Regulate Population Stability in Amazon Floodplain Fishes." *Freshwater Biology* 66(6): 1101–9. https://doi.org/10.1111/fwb.13702.

Sadoul, B., B. Geffroy, S. Lallement, and M. Kearney. 2020. "Multiple Working Hypotheses for Hyperallometric Reproduction in Fishes under Metabolic Theory." *Ecological Modelling* 433: 109228. https://doi.org/10.1016/j.ecolmodel.2020.109228.

Sandblom, E., T. D. Clark, A. Gräns, A. Ekström, L. Jeroen Brijs, F. Sundström, A. Odelström, A. Adill, T. Aho, and F. Jutfelt. 2016. "Physiological Constraints to Climate Warming in Fish Follow Principles of Plastic Floors and Concrete Ceilings." *Nature Communications* 7(1): 11447. https://doi.org/10.1038/ncomms11447.

Schoolfield, R. M., P. J. H. Sharpe, and C. E. Magnuson. 1981. "Non-Linear Regression of Biological Temperature-Dependent Rate Models Based on Absolute Reaction-Rate Theory." *Journal of Theoretical Biology* 88(4): 719–31. https://doi.org/10.1016/0022-5193(81)90246-0.

Smallegange, I. M., H. Caswell, M. E. M. Toorians, A. M. de Roos, and J. Metcalf. 2017. "Mechanistic Description of Population Dynamics Using Dynamic Energy Budget Theory Incorporated into Integral Projection Models." *Methods in Ecology and Evolution* 8(2): 146–54. https://doi.org/10.1111/2041-210x.12675.

Soetaert, K., T. Petzoldt, and R. Woodrow Setzer. 2010. "Solving Differential Equations in R: PackagedeSolve." *Journal of Statistical Software* 33(9): 1–25. https://doi.org/10.18637/jss.v033.i09.

Stearns, S. C. 1992. *The Evolution of Life Histories*. Oxford: Oxford University Press.

Swift, D. R. 1965. "Effect of Temperature on Mortality and Rate of Development of the Eggs of the Pike (*Esox lucius* L.) and the Perch (*Perca fluviatilis* L.)." *Nature* 206(4983): 528–8. https://doi.org/10.1038/206528a0.

Thorson, J. T., S. B. Munch, J. M. Cope, and J. Gao. 2017. "Predicting Life History Parameters for all Fishes Worldwide." *Ecological Applications* 27(8): 2262–76. https://doi.org/10.1002/eap.1606.

Thunell, V., A. Gårdmark, M. Huss, and Y. Vindenes. 2022. "Model Code, Data and R Scripts from "Optimal Energy Allocation Trade-off Driven by Size-Dependent Physiological and Demographic Responses to Warming"." Zenodo. https://doi.org/10.5281/zenodo.7391013.

van der Sleen, P., P. A. Zuidema, J. Morrongiello, J. L. J. Ong, R. R. Rykaczewski, W. J. Sydeman, E. Di Lorenzo, and B. A. Black. 2022. "Interannual Temperature Variability is a Principal Driver of Low-Frequency Fluctuations in Marine Fish Populations." *Communications Biology* 5(1): 28. https://doi.org/10.1038/s42003-021-02960-y.

van Dorst, R. M., A. Gårdmark, R. Svanbäck, U. Beier, G. A. Weyhenmeyer, and M. Huss. 2018. "Warmer and Browner Waters Decrease Fish Biomass Production." *Global Change Biology* 25: 1395–408. https://doi.org/10.1111/gcb.14551.

van Rijn, I., Y. Buba, J. DeLong, M. Kiflawi, and J. Belmaker. 2017. "Large but Uneven Reduction in Fish Size across Species in Relation to Changing Sea Temperatures." *Global Change Biology* 23(9): 3667–74. https://doi.org/10.1111/gcb.13688.

Vindenes, Y., E. Edeline, J. Ohlberger, Ø. Langangen, I. J. Winfield, N. C. Stenseth, and L. A. Vøllestad. 2014. "Effects of Climate Change on Trait-Based Dynamics of a Top Predator in Freshwater Ecosystems." *The American Naturalist* 183(2): 243–56. https://doi.org/10.1086/674610.

Vindenes, Y., Ø. Langangen, I. J. Winfield, and L. A. Vøllestad. 2016. "Fitness Consequences of Early Life Conditions and Maternal Size Effects in a Freshwater Top Predator." *The Journal of Animal Ecology* 85(3): 692–704. https://doi.org/10.1111/1365-2656.12489.

Wang, H. Y., S. F. Shen, Y. S. Chen, Y. K. Kiang, and M. Heino. 2020. "Life Histories Determine Divergent Population Trends for Fishes under Climate Warming." *Nature Communications* 11(1): 4088. https://doi.org/10.1038/s41467-020-17937-4.

Ward, H. G. M., J. R. Post, N. P. Lester, P. J. Askey, and T. Godin. 2017. "Empirical Evidence of Plasticity in Life-History Characteristics across Climatic and Fish Density Gradients." *Canadian Journal of Fisheries and Aquatic Sciences* 74(4): 464–74. https://doi.org/10.1139/cjfas-2016-0023.

Werner, E. E., and J. F. Gilliam. 1984. "The Ontogenetic Niche and Species Interactions in Size Structured Populations." *Annual Review of Ecology and Systematics* 15: 393–425. https://doi.org/10.1146/annurev.es.15.110184.002141.

Wieser, W., and N. Medgyesy. 1991. "Metabolic Rate and Cost of Growth in Juvenile Pike (*Esox lucius* L.) and Perch (*Perca fluviatilis* L.): The Use of Energy Budgets as Indicators of Environmental Change." *Oecologia* 87(4): 500–5. https://doi.org/10.1007/bf00320412.

Winfield, I. J., J. M. Fletcher, and J. B. James. 2013a. *Pike Fecundity Data 1963–2002*. NERC Environmental Information Data Centre. https://doi.org/10.5285/b8886915-14cb-44df-86fa-7ab718acf49a.

Winfield, I. J., J. M. Fletcher, and J. B. James. 2013b. *Pike Growth Data 1944–1995*. NERC Environmental Information Data Centre. https://doi.org/10.5285/637d60d6-1571-49af-93f7-24c1279d884d.

Winfield, I. J., and J. M. Fletcher. 2013. *Windermere Lake Temperature Data 1944–2002*. NERC Environmental Information Data Centre. https://doi.org/10.5285/9520664c-eb4d-4700-b064-5d215d23e595.

Wootton, H. F., J. R. Morrongiello, T. Schmitt, and A. Audzijonyte. 2022. "Smaller Adult Fish Size in Warmer Water Is Not Explained by Elevated Metabolism." *Ecology Letters* 25(5): 1177–88. https://doi.org/10.1111/ele.13989.

SUPPORTING INFORMATION

Additional supporting information can be found online in the Supporting Information section at the end of this article.

How to cite this article: Thunell, Viktor, Anna Gårdmark, Magnus Huss, and Yngvild Vindenes. 2023. "Optimal Energy Allocation Trade-Off Driven by Size-Dependent Physiological and Demographic Responses to Warming." *Ecology* 104(4): e3967. https://doi.org/10.1002/ecy.3967